Predictions of Land Use/Land Cover Changes, Drivers, and Their Implications for Dense Forest Degradation in Kunar Province, Eastern Afghanistan

Bilal Jan Haji Muhammad , Muhammad Jalal Mohabbat , Lia Duarte * , Ana Cláudia Teodoro

Posted Date: 6 March 2026

doi: 10.20944/preprints202603.0530.v1

Keywords: Landsat images; LCM; SVM; CA-MC model; TerrSet; Kunar province

 doi:10.20944/preprints202603.0530.v1

Article

Predictions of Land Use/Land Cover Changes, Drivers, and Their Implications for Dense Forest Degradation in Kunar Province, Eastern Afghanistan

Bilal Jan Haji Muhammad [1], Muhammad Jalal Mohabbat [2], Lia Duarte [1,3,*] and Ana Cláudia Teodoro [1,3]

[1] Department of Geosciences, Environment and Spatial Planning, Faculty of Sciences, University of Porto, 4169-007 Porto, Portugal

[2] Department of Geological Engineering and Exploration of Mines, Kabul Polytechnic University, Kabul, Afghanistan

[3] Institute of Earth Sciences, Faculty of Sciences, University of Porto, 4169-007 Porto, Portugal

* Correspondence: liaduarte@fc.up.pt

Abstract

Changes in land use and land cover (LULC) are among the leading contributors to global environmental transformation. Analyzing these dynamics is essential for understanding historical land utilization patterns and identifying the key drivers behind such shifts. This research focuses on LULC changes in the Kunar region of eastern Afghanistan. To classify the LULC types, the study area was divided into nine major classes using the Support Vector Machine (SVM) algorithm, based on Landsat 07 Enhanced Thematic Mapper Plus (ETM+) data for 2004 and Landsat 8 Operational Land Imager (OLI) data for 2014 and 2024. Past and present changes were evaluated using ArcGIS 10.8, while future scenarios for 2034 and 2044 were simulated using the Land Change Modeler (LCM) embedded in the TerrSet platform, combined with the Cellular Automata–Markov Chain (CA-MC) model with 90% kappa agreement validation value. From 2004 to 2024, grassland expanded significantly from 68.93% (3,406 km^2) to 73.94% (3,654 km^2). Built-up areas grew from 0.59% (29.10 km^2) in 2014 to 1.02% (50.39 km^2) in 2024. Conversely, dense forest cover declined from 27.50% (1,358.90 km^2) to 22.96% (1,134.75 km^2), a decrease of 224.15 km^2. Barren land, after a temporary increase, also showed a net decline. Projections for 2034 and 2044 suggest a further reduction in forested areas to 1,077 km^2, while grasslands and urbanized zones are expected to increase to 3690 km^2 and 60.63 km^2, respectively. These trends emphasize a swift transition in land use patterns, primarily driven by the conversion of forested and barren landscapes into settlements and grasslands. The findings underline the urgent need for implementing sustainable land management strategies to curb environmental degradation and ensure balanced land resource utilization in the future.

Keywords: Landsat images; LCM; SVM; CA-MC model; TerrSet; Kunar province

1. Introduction

Land use and land cover (LULC) transformations arise from a complex interplay of natural and human-induced factors, leading to significant variations in the distribution and intensity of different land categories over time. These shifts have attracted considerable global attention due to their profound influence on ecosystems, with forested landscapes being especially sensitive to such dynamics [1]. Gaining a clear understanding of LULC processes is essential for the sustainable governance of land resources, as it sheds light on the intricate interactions between land systems and human activity [2]. Human-driven and natural phenomena operating across different spatial and temporal scales shape LULC at the regional and global levels [3,4]. These changes are characterized

 doi:10.20944/preprints202603.0530.v1

by non-linear, dynamic interactions between anthropogenic activities and environmental systems, leading to complex land surface transformations.

Over the past 20 years, an evident global trend has been the expansion of built-up areas, accompanied by a significant reduction in forest cover [5–7]. Numerous studies have linked these changes to urbanization, forest-to-settlement conversions, and deforestation [8]. Comprehensive assessments of LULC dynamics have been carried out across continents, including North America [9], South America [10], Africa [11], Asia [12], and Afghanistan [13,14]. Rapid industrialization and agricultural development historically led to widespread deforestation in industrialized regions like Europe and the United States before the mid-19th century [15]. Today, rapid urban expansion, particularly in developing countries such as Afghanistan, is primarily driven by demographic and socio-economic pressures [16]. Furthermore, overexploitation of natural resources, climatic variability, and topographical diversity continue to influence the rate and nature of LULC changes [17]. These shifts are especially impactful in regions where the local economy heavily depends on forests and natural ecosystems.

Sustainable land management strategies require a thorough understanding of the human and environmental factors driving LULC changes. It is crucial to comprehend the spatial and temporal patterns of LULC and the factors that influence them, whether directly or indirectly, as such knowledge enables the projection of future scenarios [18]. Examining these drivers and modeling future changes in forest regions plays a key role in effective land use and forest management planning. Understanding past and current transformations is therefore vital for the stewardship of natural resources, such as forests [19]. Satellite-based remote sensing offers a cost-effective and dependable approach for assessing LULC changes, with Landsat data commonly used because its long-term, freely available, and consistently calibrated imagery is particularly valuable for studies in resource-limited countries [20]. Precise calibration and validation of LULC models are essential to achieve reliable future forecasts [21]. Land Change Modeler (LCM) is widely employed in environmental studies to map and simulate LULC shifts over time and space [22]. These models vary in approach, some are spatial or non-spatial, static or dynamic, inductive or deductive, and may be pattern-based or agent-driven [23,24]. The LCM helps visualize LULC alterations over time using statistical analyses and graphical representations, while the Cellular Automata-Markov Chain (CA-MC) model is applied for predicting future land use patterns [25]. This model, which is inherently probabilistic, utilizes pairs of historical satellite images to estimate land transition probabilities [26]. It allows for accurate simulation of land cover transitions by analyzing the shift of spatial units (cells) between LULC classes, incorporating relevant socio-economic and environmental variables [27]. The model's effectiveness is evaluated by comparing predicted land cover maps with actual observations, enabling validation and refinement of predictions. These validated outcomes are then used to interpret past transformation drivers and simulate future scenarios.

Natural resource distribution, condition, and management exhibit significant variability across Afghanistan [13,14]. The country is highly vulnerable to environmental disturbances caused by natural phenomena and human activities. Kunar Province, located in eastern Afghanistan, constitutes a critically important and ecologically diverse forested region within the country [28]. However, it faces serious challenges, including unchecked urbanization, environmental degradation, soil erosion, reduced agricultural productivity, and widespread deforestation [29]. Understanding the patterns and causes of LULC change in this area is critical for developing effective environmental management strategies. Despite numerous global studies on LULC [7,22,27], Kunar remains relatively underexplored, despite severe ecological and social pressures. This research aims to bridge that gap by addressing the following key questions: (i) What types of LULC changes have occurred in the Kunar area from 2004 to 2024, and which land cover categories were most affected? (ii) What are the expected trends and patterns of change in the future 2034 to 2044? (iii) What factors influence LULC transformations in the region? (iv) How do LULC changes affect the future of dense forests in the study area? Exploring these questions is essential for understanding the socio-economic and environmental mechanisms driving land change, and mitigating deforestation and ecological

 doi:10.20944/preprints202603.0530.v1

degradation in Kunar. Accurate forecasting of these dynamics supports the formulation of informed land use policies. The outcomes of this study will provide empirical evidence of LULC dynamics in Kunar, identify key contributing factors, and offer policy recommendations for sustainable land management and planning.

2. Materials and Methods

2.1. Study Area

In eastern Afghanistan, Kunar province spans approximately 4,942 km² and lies at approximately 35° 00′ 0.00″ N and 71° 12′ 0.00″ E (Figure 1). The region is predominantly mountainous and forest-covered, sharing boundaries with Nangarhar, Nuristan, and Laghman provinces, and with Pakistan on the eastern frontier. Its southwestern portion intersects with the Nuristan-Kunar tectonic belt, located near coordinates 34°N and 70°E, and rises to an average elevation of about 4,428 meters above sea level [30,31]. The area's rugged topography, characterized by deep valleys and high mountain ridges, has played a vital role in shaping its ecological setting and socio-economic structure [30,32]. Kunar experiences varied climatic conditions, with an annual mean temperature of around 20 °C. Most of its rainfall, averaging roughly 469 mm per year, falls between November and May, marking the primary wet season. Summers tend to be arid, with peak temperatures in July soaring to nearly 40 °C, while winter months, especially January, can present temperatures dropping to around 2 °C. This broad range in temperature and precipitation directly affects vegetation cycles and land utilization patterns.

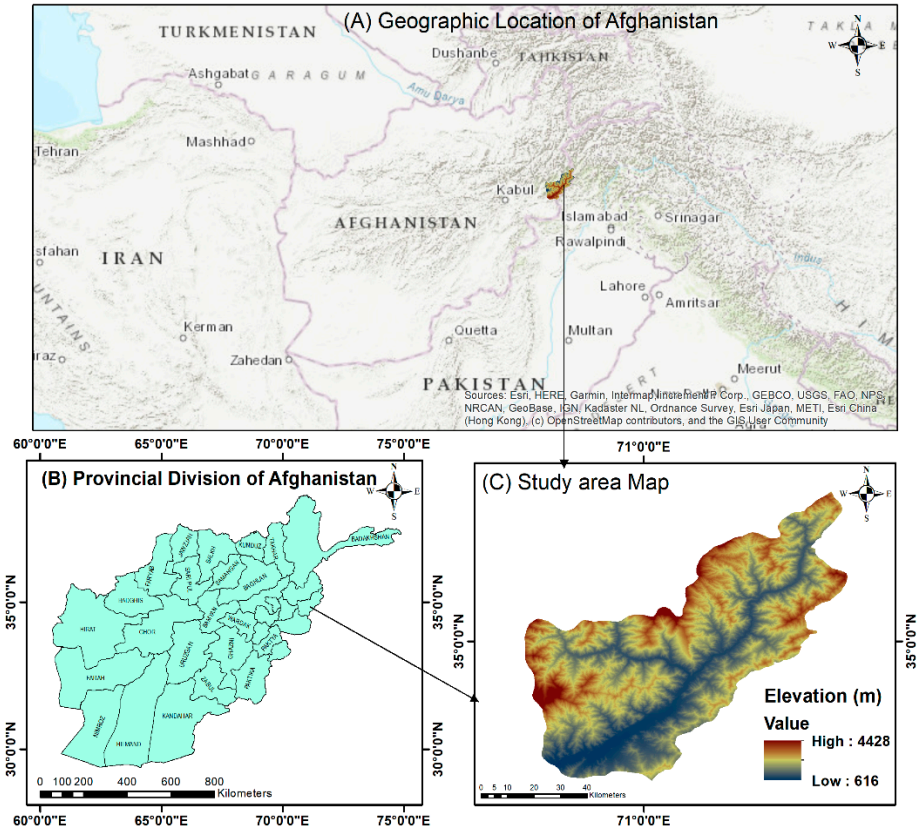

Figure 1. Geographic context and study area representation. (A) Strategic geographic location of Afghanistan within South and Central Asia, (B) Provincial boundaries of Afghanistan, and (C) Elevation map of Kunar Province highlighting the study area.

Geologically, the area includes a complex mix of rock types, including dolerite, basalt, and rhyolite, alongside unconsolidated alluvial and colluvial sediments [30]. These geological features,

 doi:10.20944/preprints202603.0530.v1

combined with abundant natural resources such as timber and fertile soil, form the backbone of the province's economy and underscore its strategic environmental significance [28]. The province's varied ecosystems and rich biodiversity make it an ideal setting for monitoring LULC transformations. Forest-related activities dominate the local economy and are a primary source of livelihood for its residents, underscoring the critical role of sustainable forest management in regional development and ecological stability.

2.2. Sources and Data Types

The study relied on a combination of different spatial datasets, including satellite imagery, digital elevation models (DEM), and field-collected data. Specifically, two cloud-free Landsat 7 and Landsat 8 satellite images were sourced from the United States Geological Survey (USGS) platform (http://glovis.usgs.gov/), with acquisition dates of November 15, 2003 (Table 1). In addition, a 30-meter resolution DEM was downloaded from OpenTopography (https://opentopography.org/). This DEM was used to delineate the study area's boundaries, analyze topographic features, generate elevation profiles, and calculate slope gradients. The remote sensing component utilized Landsat 7 Enhanced Thematic Mapper Plus (ETM+) data from 2004 and Landsat 8 Operational Land Imager (OLI) data from 2014 and 2024. Both image sets were captured during Afghanistan's dry season in November to ensure optimal atmospheric conditions, minimize cloud interference, and maintain consistent surface reflectance values across periods. Ground-truthing activities were conducted using Global Navigation Satellite System (GNSS) devices at selected Ground Control Points (GCPs) to validate satellite-based interpretations. During field visits, LULC categories were recorded, and photographic evidence was collected to support classification accuracy and consistency in interpretation.

Table 1. Landsat data utilized to analyze the LULC in the study area.

Satellite	Path/Row	Data Acquisition	Resolution	Year
Landsat 7 ETM+	151/35 152/36	15-Nov-04	30 m	2004
Landsat 8 OLI	151/35 152/36	14-Nov-14	30 m	2014
Landsat 8 OLI	151/35 152/36	17-Nov-24	30 m	2024

2.3. Assessment of Changes in LULC

2.3.1. Classification of Images

The classification stage is a critical component in the preparation of LULC datasets. This study used the preprocessed Landsat imagery to generate LULC maps, categorizing the landscape into nine distinct classes (Table 2). Generally, classification methods fall into two main types: supervised and unsupervised. Among these, supervised classification is often considered more effective for quantitative analysis of remote sensing data, as it relies on known training samples. In contrast, unsupervised classification groups image pixels into classes without prior training data [33]. For this research, the Support Vector Machine (SVM) algorithm, a robust machine learning approach, was employed within the Google Earth Engine (GEE) environment to classify all Landsat images. Following classification, change detection and the creation of transition matrices were carried out. These calculations were performed using ArcGIS 10.7 and TerrSet software [34], ahead of the future projection phase. The transition and change matrices were derived by comparing classified images from two different time points, such as 2004 and 2024, and similarly for other selected periods.

 doi:10.20944/preprints202603.0530.v1

Table 2. Key LULC Types and Their Characteristics.

LULC Classes	Characteristics
Water	Areas comprising rivers, channels, ponds, lakes, and essential dams or reservoirs.
Dense Forest	Regions dominated by a dense collection of trees, including both deciduous and evergreen forests, as well as mixed woodlands.
Shrubs	Areas featuring a variety of small to medium-sized plants, often ornamental or garden varieties.
Cropland	Land used for cultivating both perennial and annual crops, including irrigated fields, rural farms, and commercial agricultural operations, such as sesame and sugarcane farming.
Built-Up Land	Urban and industrial zones, including commercial spaces and residential areas, both in cities and rural regions.
Barren Land	Land that is desolate, infertile, and arid, with little or no vegetation.
Snow	Area covered by accumulated frozen precipitation.
Open Forest	Regions with a sparse tree cover, where the canopy is light and the woodland is less dense.
Grassland	Expansive, flat areas covered primarily by grasses, often forming plains or meadows.

2.3.2. Accuracy Evaluation

Accuracy assessment is a critical step to determine how well the classified image represents real-world conditions. Since maps generated by image classification often contain errors, validating their accuracy is essential to build confidence in the results and provide a solid foundation for monitoring future land cover changes. This study validated the classified maps against reference data from multiple sources, including Landsat imagery, Google Earth, historical reports, and field surveys. The error or confusion matrix is the most common and reliable method for assessing classification accuracy. This matrix provides detailed statistics, including user accuracy, producer accuracy, overall classification accuracy, and the kappa coefficient. The kappa statistic was calculated following a specific formula (Equation 1) outlined of [35]. Based on the interpretation by [23], a kappa value below 40% indicates poor agreement, between 40% and 80% moderate agreement, and values exceeding 80% indicate strong and reliable classification results.

The results show consistently high classification performance across all three study years. The overall accuracy values were 97.20% (2004), 97.01% (2014), and 97.40% (2024), while the corresponding kappa coefficients were 96.80%, 96.70%, and 97%, respectively (Table S1). These values indicate a very strong agreement between the classified maps and the reference data, confirming the reliability and robustness of the LULC classification results for subsequent change detection and analysis.

$$K = \left(\frac{N\sum_{i=1}^{r} Xii - \sum_{i=1}^{r}(Xi+)*(X+i)}{N^2 - \sum_{i=1}^{r}(Xi+)*(X+i)}\right) \times 100 \quad (1)$$

In this context, r signifies the total number of rows within the confusion matrix. Xii corresponds to the number of correctly classified instances, represented by the diagonal elements. $X+i$ and $Xi+$ denote the marginal totals for row i and column i, respectively. N represents the overall number of observations utilized in the accuracy assessment.

2.3.3. Change Detection

The rapid expansion of large-scale data storage capabilities has led to the development of numerous numerical change-detection techniques over recent decades, aimed at estimating and monitoring LULC changes [36]. Among the most widely employed techniques for change detection are image differencing, image segmentation, Principal Component Analysis (PCA), Change Vector Analysis (CVA), and post-classification comparison [37]. Recent advances have led to growing interest in using machine learning to analyze and interpret remote sensing data [38,39]. The present study examined spatial changes in the study area using a change detection approach that integrated

 doi:10.20944/preprints202603.0530.v1

ArcGIS tools with Earth Resources Data Analysis System (ERDAS) image analysis capabilities (Hexagon Geospatial. ERDAS IMAGINE® Software; Hexagon Geospatial: Norcross, GA, USA). For each LULC category, the area expressed in km² was computed for 2004–2014 and 2014–2024, and cumulatively for 2004–2024, to thoroughly assess the landscape dynamics over time. Although various methodologies were applied to compute the LULC statistics, the change analysis fundamentally relied on the differences between the classified datasets from 2004, 2014, and 2024. Additionally, the Magnitude of Change (MC) and Annual Rate of Change (ARC) [40] were derived using specific equations to quantify and interpret the extent and pace of land cover transformation (Equations (2) and (3)).

$$MC\ (\mathrm{km}^2) = Af - Ai \quad (2)$$

$$ARC\ (\mathrm{km}^2\mathrm{year}^{-1}) = \frac{Af - Ai}{n} \quad (3)$$

where, Ai represents the area (in km²) of a given class at the beginning of the study period, Af denotes the area (in km²) of the same class at the end of the study period, and n refers to the total number of years covered by the analysis.

2.4.5. Annual Rate of Change Analysis

The ARC for each land use category is calculated as the difference between the final and initial years, reflecting the overall magnitude of change. This difference is then divided by the initial year's area and the duration of the study period. To quantify the spatiotemporal extent and the rate of change in LULC classes, Equation (4) was applied:

$$ARC\ (\%) = \frac{Af - Iy}{Iy * t} * 100 \quad (4)$$

where, ARC represents the annual rate of change within the LULC categories, Iy and Af denote the areas at the initial and final years, respectively, and t indicates the length of the time interval.

2.4. LULC Drivers

LULC changes are influenced by natural processes and human activities [41]. Large-scale transformations at global and regional levels significantly impact various ecological systems. If the key drivers of change identified in the past persist, it is reasonable to expect they will continue to shape future landscapes [27]. In LULC change modeling, topographic and proximity-related variables are frequently employed as influential factors. Variables such as elevation, slope, distance to roads, and distance to buildings were selected as potential driving forces. Additionally, distances to roads and rivers were treated as dynamic variables to account for their temporal variations across the study period (Figure 2).

2.5. Change Analysis and Modeling

2.5.1. LCM-Based Post-Classification Analysis

Various modeling tools have been applied to investigate LULC dynamics, each offering varying degrees of predictive accuracy [42]. The LCM, CA, and CA-Markov models are among the more commonly used tools integrated within TerrSet software. For short-term projections, generally covering periods of ten years or less, LCM has demonstrated high predictive reliability in LULC change analyses [43]. Furthermore, LCM often outperforms other models based on supervised classification methods, mainly due to the strength of its multi-layer perceptron (MLP) neural network framework [44]. These advantages supported the decision to employ LCM to predict LULC changes within the study area, targeting the year 2044. Using LCM, scenario maps, and LULC change analyses for the study area were generated through a sequence of steps, including change analysis, transition potential modeling, model validation, and change prediction. The model compares two sets of classified images that share the same thematic legends and spatial resolutions, producing outputs that allows to analyze changes [45]. This study assessed LULC changes across two-time intervals, 2004–2014 and 2014–2024, using the post-classification comparison technique, a widely recognized

 doi:10.20944/preprints202603.0530.v1

method for detecting LULC transformations [46]. The change detection module within LCM was employed to quantify various aspects of change, including gains and losses in each LULC class, the net change (calculated as the difference between gains and losses), contributions of each class to the net change, and the transition pathways between different LULC categories across the specified periods [47].

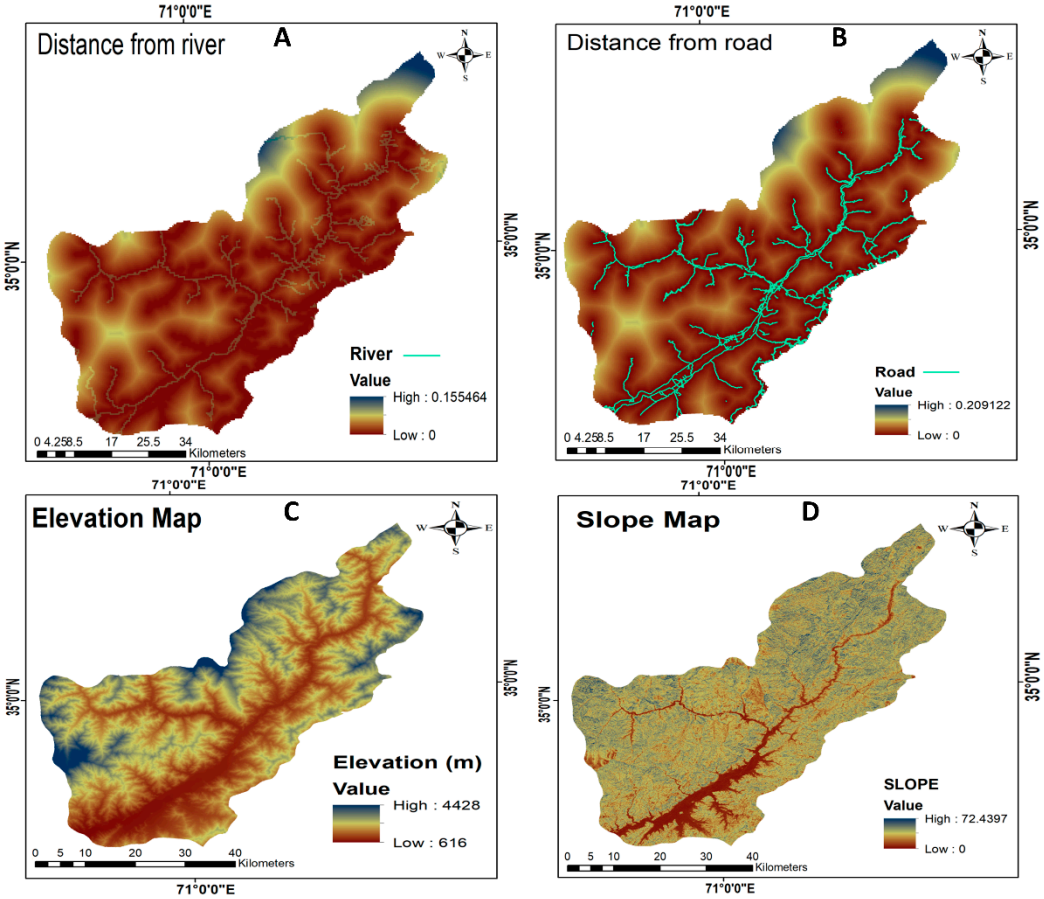

Figure 2. Study area suitability maps were generated using several input datasets, including proximity to rivers (A), proximity to roads (B), DEM data (C), and slope information (D). These datasets were sourced from OpenTopography at https://doi.org/10.5069/G9445JDF.

2.5.2. Simulation of Transition Potentials Using an MLP Neural Network

The LULC maps of the years (2004–2014 and 2014–2024) were used as inputs to create the transitions. Using the change analysis module, dominant transitions (dense forest to grassland, cropland to built-up area) were identified, which were used to create potential transition maps for modeling by setting a threshold of 1000 hectares. The change maps were used to estimate the probability of conversion from other classes to cropland. The LCM uses logistic regression, SimWeight, and an MLP as modeling algorithms to model transition variables. This study used the MLP neural network to construct the transition potential maps. The MLP neural network operates as a feedforward artificial neural network (ANN) model with a unidirectional data flow through hidden layers in between. Neural network training is based on a supervised training algorithm, a common method for training ANNs. The transition potential maps for the LULC changes were generated with an MLP accuracy rate (89%), which is within the acceptable range.

2.5.3. LCM Validation and Change Projection

Once the model is developed, the resulting simulation map must undergo a validation process to assess the accuracy of its predictions. Validation is a crucial step in land use forecasting. The

 doi:10.20944/preprints202603.0530.v1

validation module involves a comparative analysis of the simulated and actual land use maps, utilizing the Kappa index. However, unlike traditional Kappa statistics, this method breaks down the validation into distinct components, each with its specific Kappa metric, such as K-location, K-no, K-standard, and others. The model's outcomes are compared to the real-time land_use map for the relevant period. To assess the accuracy of the projected LULC map for 2044, the Index of Agreement (KIA) approach is applied, a common method for validating LULC change predictions [48]. This step is essential before applying the CA-Markov model to forecast land use changes over the next 20 years. To achieve this, the validation module in TerrSet Software is employed.

2.5.4. LULC Simulation and Prediction

Markov Chain Model-Based Analysis

The Markov chain model is a prominent and commonly employed tool for modeling LULC, treating the process as stochastic [49]. In a Markov system, the future state of the land use system is determined by its current state, with transitions between states representing changes in the system. The probability of such transitions occurring is referred to as the transition probability. The TerrSet model employs the CA-MC methodology, a stochastic modeling approach, to simulate future land cover changes based on historical data analysis [50]. The Markov matrix model applies Bayes' equation (5) to evaluate changes by comparing initial (T1) and subsequent (T2) land cover datasets [26].

$$\mathbf{S(t+1)} = \boldsymbol{Pij} * \mathbf{S(t)} \quad (5)$$

$$\boldsymbol{Pij} = \begin{vmatrix} \boldsymbol{P11} & \boldsymbol{P12} \ldots & \boldsymbol{P1n} \\ \boldsymbol{P21} & \boldsymbol{P22} \ldots & \boldsymbol{P2n} \\ \boldsymbol{Pn1} & \boldsymbol{Pn2} \ldots & \boldsymbol{Pnn} \end{vmatrix} \quad (6)$$

The transition probability matrix, where $\mathbf{0} \leq \mathbf{Pij} < \mathbf{1}$, and the sum $\sum_{j=1}^{n} \boldsymbol{Pij} = \mathbf{1}\ \boldsymbol{for}\ \boldsymbol{i,j} = \mathbf{1,2,} \ldots \boldsymbol{n}$, (equation 6) governs the probabilistic relationships between land cover states in the CA model. The transformation rule of the cellular states within local space is given by $\boldsymbol{f}$, and $\boldsymbol{S}$ refers to the set of discrete, finite cellular states. The transition probability matrix, $\boldsymbol{Pij}$, defines the likelihood of transitioning from one state to another. The CA-Markov model integrates various constraints and characteristics to create a unified suitability map [51]. It generates both transition probability regions and a transition probability matrix, which indicates the likelihood of a specific LULC class shifting to another. Additionally, the transition area matrix quantifies the anticipated pixel count expected to transition from each LULC class over a defined time [26].

Cellular Automata (CA)

The CA model is a local interaction-based change model that simulates system evolution by treating space and time as discrete components, typically representing space through a regular two-dimensional grid. By carefully defining transition rules, CA models are highly effective in capturing the temporal and spatial complexity inherent in LULC systems. They offer valuable insights into understanding patterns and processes, such as the development of forest structures [52]. As a bottom-up dynamic framework, CA operates within a spatiotemporal computational environment, where space and time are discretized, allowing for the simulation of intricate spatiotemporal dynamics. The state of each cell at time $\boldsymbol{t+1}$ depends on its current state and the states of its neighboring cells at a time $\boldsymbol{t}$, based on predefined transition rules. A typical CA model comprises cells, the cell space, neighborhoods, transition rules, and time steps. The neighborhood identification process utilizes a filter approach [53], where cells closer to the target cell are assigned higher weight factors. These weights, combined with transition probabilities, predict the future states of neighboring cells. As modeled by CA, land use transformations are not entirely random events. In this study, each land use cell was represented within a cellular network, surrounded by eight neighboring cells. The state of each cell indicated its land use category, and the simulation covered 20 years. The modeling adopted both the maximum transition probability rule and a hysteresis rule, ensuring that once a

 doi:10.20944/preprints202603.0530.v1

land use type was assigned to a cell, it remained unchanged throughout the simulation period [54,55] (Equation 7).

$$S(t, t+1) = f[S(t), N] \quad (7)$$

where, $S(t)$ and $S(t+1)$ represent the system's state at times (t) and $(t+1)$, respectively, while N denotes the cellular field.

3. Results and Discussion

3.1. Current Status of LULC

During the study period from 2004 to 2024, nine major LULC categories were identified (Figures 3 and 4). In 2004, grasslands dominated the study area, covering approximately 68.93% of the area, followed by dense forest 27.50%, cropland 1.23%, built-up areas 0.85%, and water bodies 0.68% (Table S4). By 2014, a notable shift had occurred: dense forest cover had decreased to 24.17%. During the same year, grassland and barren land expanded to 72.63% and 0.6%, and snow decreased to 0.06%, cropland and water bodies remained relatively stable at 1.21% and 0.64%. By 2024, the transformation of the landscape had become even more pronounced: grassland increased sharply to 73.94%, and dense forest dropped to 22.96%. Shrubs remained almost unchanged at 0.0%, but built-up land experienced substantial increases, rising to 1.02% respectively. Throughout the entire study period, grassland was significantly expanded primarily at the expense of forested areas (Figure 3D and C). Specifically, dense forest coverage declined by approximately 1358.90 to 1134.75 km², and grassland areas increased from 3406.22 km² to 3654.11 km² between 2004 and 2024 (Table S2). These trends highlight the ongoing pressure on natural ecosystems due to deforestation and urban development.

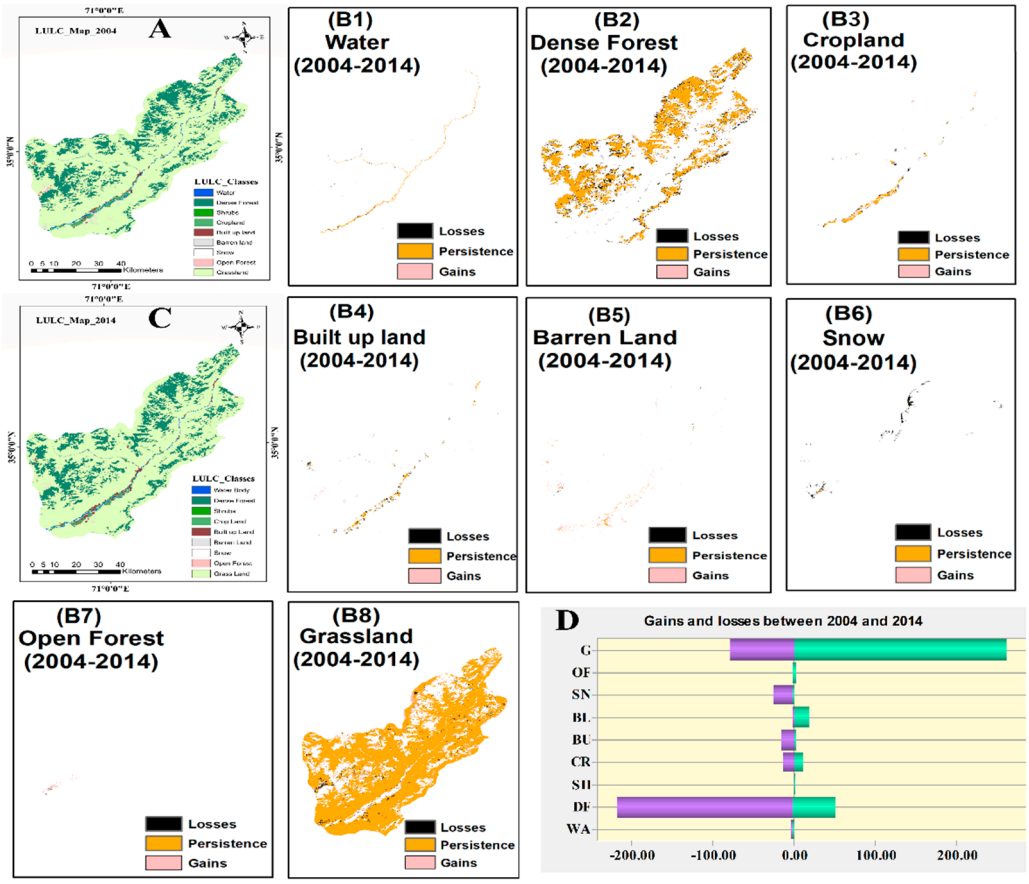

Figure 3. Analysis of LULC dynamics between 2004 and 2014. (A) LULC classification map for 2004. (C) LULC classification map for 2014. Panels (B1–B8) illustrate the change trajectories for individual land cover classes, Water (WA), Dense Forest (DF), Shrubs (SH), Cropland (CR), Built-up Land (BU), Barren Land (BL), Snow (SN),

 doi:10.20944/preprints202603.0530.v1

Open Forest (OF), and Grassland (G), highlighting areas of gain, loss, and persistence over the 10 years. (D) Comparative visualization of total gains and losses for each land cover class.

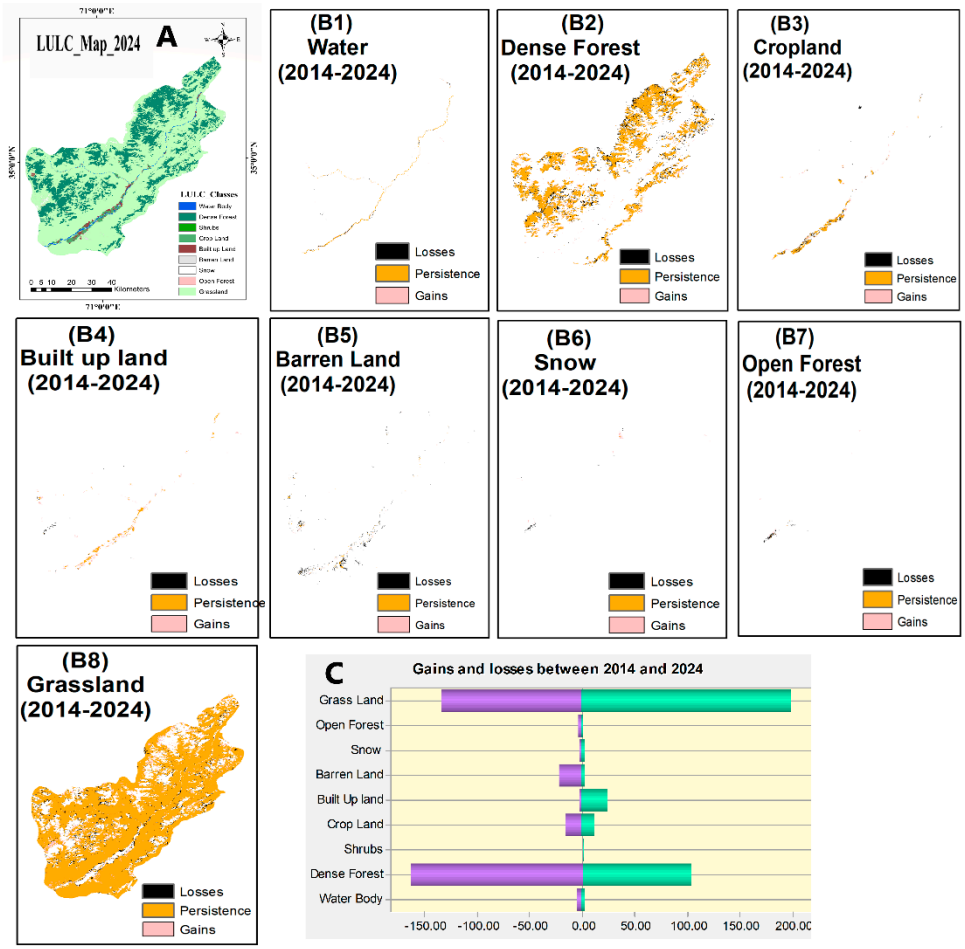

Figure 4. LULC dynamics and transition analysis in the study area from 2014 to 2024. (A) LULC classification map for the year 2024. (B1–B8) Spatial distribution of LULC transitions showing areas of losses, persistence, and gains for individual classes during the 2014–2024 period. (C) Gains and losses in area (km²) for each LULC class between 2014 and 2024.

3.2. LULC Conversions Analysis

The assessment of LULC changes was initiated using 2004 as the baseline year. Two major LULC transitions were recorded during two main periods: 2004–2014 and 2014–2024. The results of the conversion analysis highlighted substantial gains and losses across different LULC classes during both intervals (Figure 3A and 4C). Significant transformations were observed, particularly in dense forests and grassland, which underwent notable conversions into other LULC types throughout the two study periods. Dense forest areas exhibited a considerable reduction, with approximately -164.22 km² converted by 2004-2014, and -59.91 km² by 2014-2024. Similarly, snow transitioned into other land use categories, amounting to losses of -23.86 km² in 2004-2014. Cropland areas also experienced dynamic shifts, with -1.13 km² converted by 2004-2014, and -3.62 km² by 2014-2024. Built-up land conversions of -13.12 km² in 2004-2014, 21.29 km² in 2014-2024. Barren land increased 17.84 km² in the first decade, then decreased to -18.46 km² in 2014-2024. Shrubs, are relatively stable compared to other categories. Water bodies had minor conversions of -2.24 km² in 2004-2014, and -1.71 km² in 2014-2024. The open forest increased by 3.77 km² in the first period of the study, then decreased to -3.28 km² in the second period. Table S3 shows that five LULC categories, water bodies, dense forest, cropland, barren land, and snow, exhibited negative changes from 2004 to 2024. Specifically, losses were calculated at -3.95 km² for water bodies, -224.14 km² for dense forest, cropland -4.75 km², barren land

 doi:10.20944/preprints202603.0530.v1

-0.62 km², and -23.20 km² for snow. Correspondingly, the percentage for these categories was recorded at -0.08%, -4.53%, -0.09%, -0.01%, and -0.46%, respectively, reflecting the ongoing decline in natural land cover over the two decades.

3.3. Driver Variables Influencing LULC Changes

The factors driving LULC changes were identified through spatial analysis and integrated into the model as static or dynamic components. Predicting future LULC patterns in the study area was based mainly on variations in these driver effects. This study selected topographic attributes and proximity-related factors to investigate the drivers of LULC transformations. Before incorporating these variables into the model, their explanatory power was assessed using Cramer's V statistics and p-values (Table S4). Although a high Cramer's V value does not definitively confirm that a specific variable is the primary cause of LULC changes, it is a practical tool for evaluating the relative importance of each factor. When Cramer's V values are low, index probability analysis is recommended to capture the spatial distribution of different LULC types across regions. This approach allows for a quantitative understanding of pixel-level variability, particularly in areas experiencing shifts between cropland and other land types (often called disturbance zones). The results (Table S4) indicated elevation, slope, distance to rivers, and distance to roads were critical in explaining LULC transitions. Among these, slope exhibited lower Cramer's V values, suggesting that its influence on land cover change in the study area was relatively minor. Conversely, variables with higher Cramer's V values were identified as significant contributors to LULC dynamics. Topographic factors, particularly elevation and slope, emerged as dominant influences on the spatial extent of built-up areas, vegetation distribution, forest cover, and the conversion of forests into grassland. As [56] found, deforestation rates tend to decline as slope steepness increases. In lowland regions, accessibility, facilitated by proximity to rivers and roads, was a key factor driving the expansion of grasslands and agricultural. These accessibility factors significantly contributed to land-use changes by easing human access to natural resources and accelerating land transformation processes.

3.4. LULC Transition Probability Matrix (TPM)

The transition potential model (TPM) assesses the likelihood of LULC transitions from one class to another, based on the suitability of specific regions and the influence of driving forces [57]. The TPM captures the probability of each land use class shifting to another, as a crucial tool for LULC change predictions [58]. In this study, model-generated TPMs were developed for 2004–2014 and 2014–2024, as shown in (Table S5). The spatiotemporal dynamics between earlier and later land cover maps were systematically recorded using cross-tabulation, quantifying both the degree of change and the conversion between various land cover types. In the cross-tabulation matrices (Table S5), the bolded diagonal indicates the probability that each LULC class remains unchanged between the periods. Grassland exhibited the highest stability among all classes, with 3406.22 km² projected to persist as grassland from 2004 to 2024. Significant transformations were observed following the conversion of dense forest to grassland, as deforestation has been the primary driver of dense forest decline, leading to a notable expansion of grassland areas. Meanwhile, water bodies experienced notable shifts, transforming into grasslands, cropland, and built-up/barren lands. However, minimal reversion of built-up/barren lands, 0.08 km², and 0.34 km², back into water bodies was recorded. Over the entire study period (2004–2024), the most significant net loss was the conversion of dense forest to grassland, amounting to 3589.12 km². Historically, the lowland areas were also dominated by forests before 2004 and 2014. However, intensive deforestation and expansion of built areas have led to a sharp decline in the natural cover. More recently, built-up areas have been expanding continuously and rapidly. Similar patterns were reported in China, where [59] found that the conversion of forest and cropland primarily drove the expansion of urban built-up areas. [60] further emphasized that effective urban planning is essential to manage the challenges of rapid urban growth, including competing land and water demands at the urban fringe.

 doi:10.20944/preprints202603.0530.v1

3.5. LULC Gains and Losses (2004–2024)

The patterns of LULC gains and losses in the study area over the 20 years are illustrated in Figures 3B1-B8, 3D, 4B1-8, and 4C. The LULC changes reveal highly contrasting transformations, where pink shades represent the area gained (in km²) per category, and black-colored shades depict the corresponding losses. As shown in Figure 3D, between 2004 and 2014, grassland expanded by approximately 261.63 km² and barren land expanded by 18.81 km². During this time, dense forest and snow declined by roughly -216.81 km² and -25 km², respectively. No significant changes were observed in the water bodies, open forest, shrubs, and cropland categories. In the second timeframe (2014–2024), grassland registered a further gain of 199.28 km². Conversely, cropland, barren land, and dense forest showed notable reductions of around -15.7 km², -21.86 km², and -163.04 km², respectively (Figure 4C). These findings align with Veldman's (2016) observations that the savannah forest ecosystem is increasingly under threat from multiple pressures. Key factors driving forest degradation include the extraction of firewood, uncontrolled bushfires, timber extraction, and illegal mining activities.

3.6. Contributors to LULC Changes from 2004 to 2024

A series of contributor plots was generated to analyze the transformation of various LULC classes into dense forest, illustrating the dynamics of dense forest expansion over 20 years in km². The data reveal that grassland was the primary source of driving the reduction in dense forest. Between 2004 and 2014, approximately 160 km² of dense forest and 3 km² of barren land were converted to grassland (Figure 5A). From 2014 to 2024, dense forest was further reduced, contributing to the grassland by around 59 km² (Figure 5B). From 2014 to 2024 about 59 km² of dense forest and 2.9 km² of barren land were transformed into grassland. From 2004 to 2024 dense forest remained the dominant contributor to grassland expansion, supplying approximately 160 km² and 59 km², respectively.

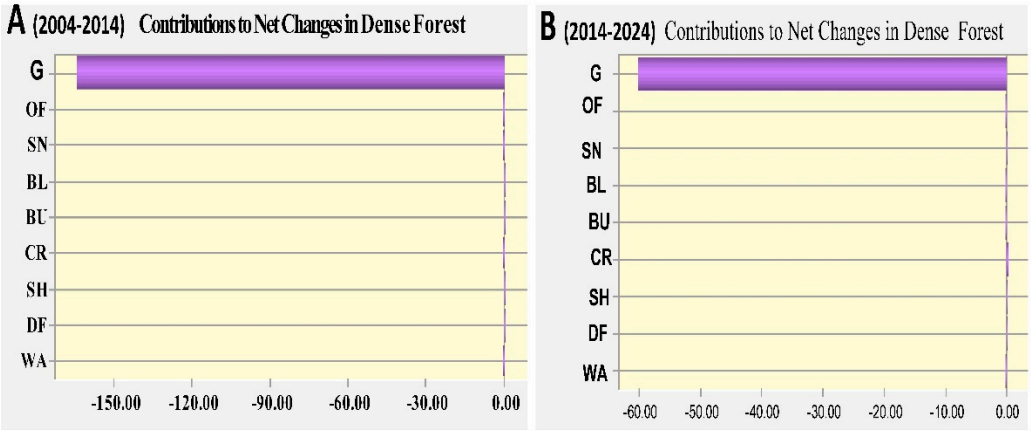

Figure 5. Contributions of different LULC types to the net loss of dense forest from2004 to 2024, with grassland showing the most significant impact.

3.7. Model Validation

A validation process was conducted by comparing the actual and simulated LULC maps for 2024. The validation outcomes, summarizing the model's performance, are detailed in (Table S4). The accuracy assessment involved comparing the predicted LULC of 2024 with the classified map for the same year. The validation metrics reveal that the Kno value is 0.91, Klocation is 0.92, and the overall Kappa statistic (K-standard) stands at 0.9143. These results indicate that the model demonstrates a high capability in accurately predicting the location and quantity of land cover changes, with minimal spatial and quantitative errors. All K-index values surpass the minimum acceptable threshold of 83%,

 doi:10.20944/preprints202603.0530.v1

as recommended by [61]. Furthermore, the Kappa values recorded in this study exceed 90%, reflecting a strong agreement between the predicted and actual 2024 maps confirming the model's robust predictive power for future LULC scenarios, making it reliable for projections for 2034 and 2044 (Table 3). The landscape prediction in this study is driven by the influence of selected spatial factors, including proximity to roads and rivers, slope, and elevation (Table 4).

Table 3. Shows the K-index values for the 2024 simulated LULC map.

Index Value	Index Value
K no	0.9116
K Location	0.9220
K standard	0.9143

Table 4. Displays the driver factors and their assigned weights.

No	Factors	Weight (%)
1	Distance to the roads	0.23
2	Distance to the river	0.23
3	Slope	0.17
4	Elevation	0.17

A visual comparison between the 2024 LULC map and the simulated map (Figure 6) reveals a strong resemblance (Table 5). The overlapping areas across all land use categories between the actual and simulated maps fall within an acceptable range, with differences in area for each LULC type remaining under 5%. Despite some variability in the classified land use types, the overall change trends show strong agreement between the historical LULC transitions and the predicted outcomes. This high consistency between the current and simulated spatial distributions confirms that the developed CA-Markov model is highly reliable for forecasting future LULC changes in the study area for the years 2034 and 2044.

Table 5. LULC change prediction validation based on the actual and simulated 2024 LULC.

LULC Types	Simulated 2024	Current 2024
	Area (km²)	Area (km²)
Water	28.401	29.71
Dense Forest	1134.75	1134.75
Shrubs	0.0677	0.07
Cropland	53.2613	56.26
Built-Up Land	49.895	50.39
Barren Land	10.7161	11.36
Snow	3.6147	3.614
Open Forest	1.5516	1.55
Grassland	3652.112	3654.11

3.8. Predictive Analysis of LULC Dynamics

The predicted LULC types for 2034 and 2044 were estimated using the CA-Markov model, with results shown in (Table S6). The dense forest area is projected to decrease from 1134.75 km² in 2024 to 1123.22 km² in 2034, and further decrease to 1077.65 km² in 2044. Built-up, and bare land, are expected to steadily increase, with built-up area expanding from 52.16 km² in 2034 to 60.63 km² in 2044, bare land growing from 24.2 km² in 2024 to 2044, and open forest increasing 4.57 km² from 2024 to 2044. Conversely, water bodies and shrubs are anticipated to decline slightly from 29.06 km², 0.07 km² in 2034 to 28 km², 0.01 km² in 2044. The increase in grassland, built-up area, and bare land will come at the expense of dense forest and cropland, which will experience the most considerable losses

 doi:10.20944/preprints202603.0530.v1

between 2024 and 2044 (Figures 8A, 8B1-B8, 8C). Specifically, dense forest will lose approximately 11.53 km² and 41.14 km², respectively, with the water body and snow showing the least loss. Grassland is expected to experience the highest gain in this period (Figures 7A, 7B8, 7C).

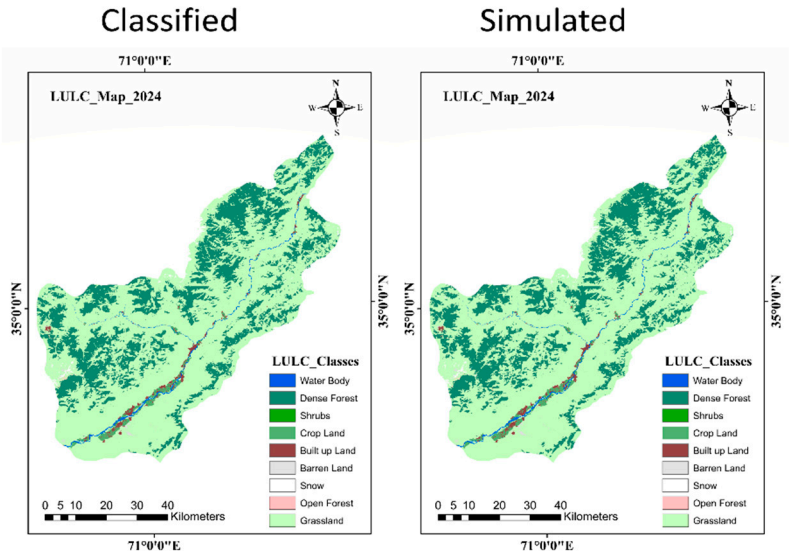

Figure 6. Current and Simulated LULC maps of 2024.

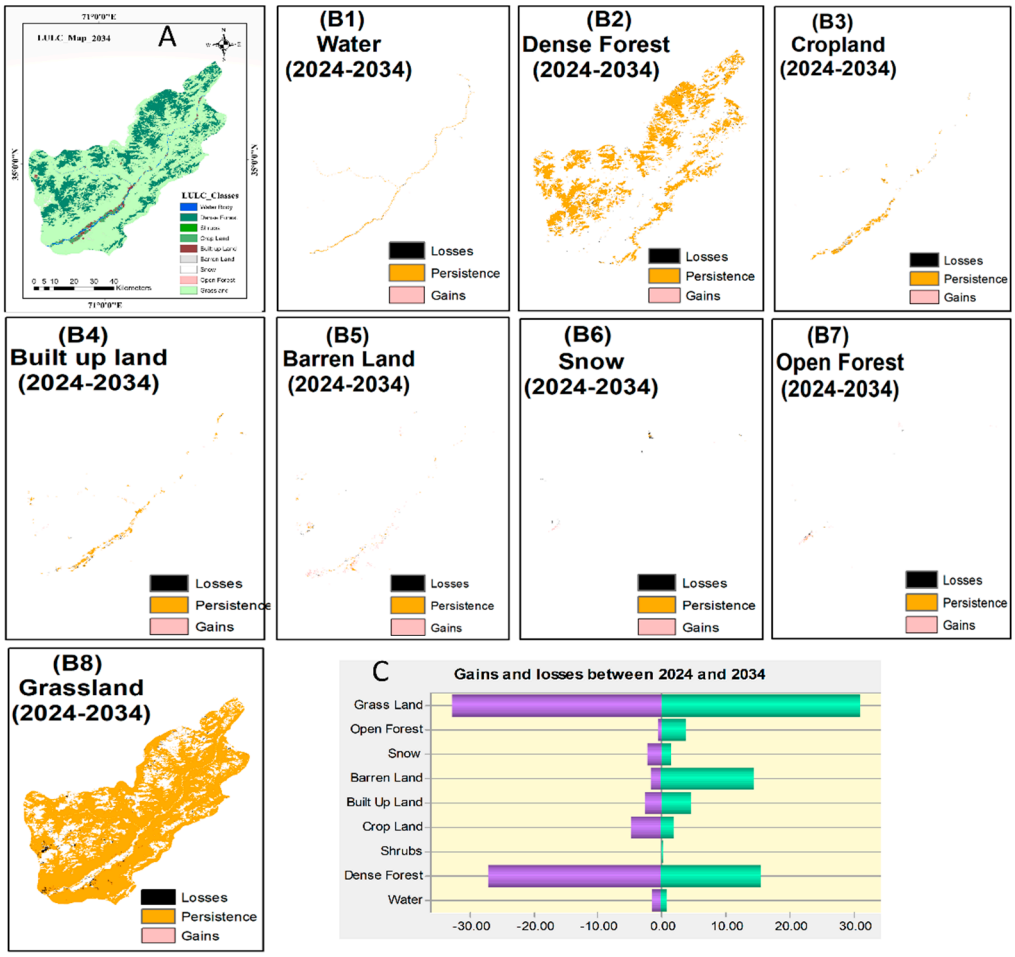

Figure 7. LULC dynamics and transition analysis in the study area from 2024 to 2034. (A) LULC classification map for the year 2034. (B1–B8) Spatial distribution of LULC transitions showing areas of losses, persistence, ad

 doi:10.20944/preprints202603.0530.v1

gains during the 2024–2034 period. (C) Gains and losses in area (km²) for a single LULC class between 2024 and 2034.

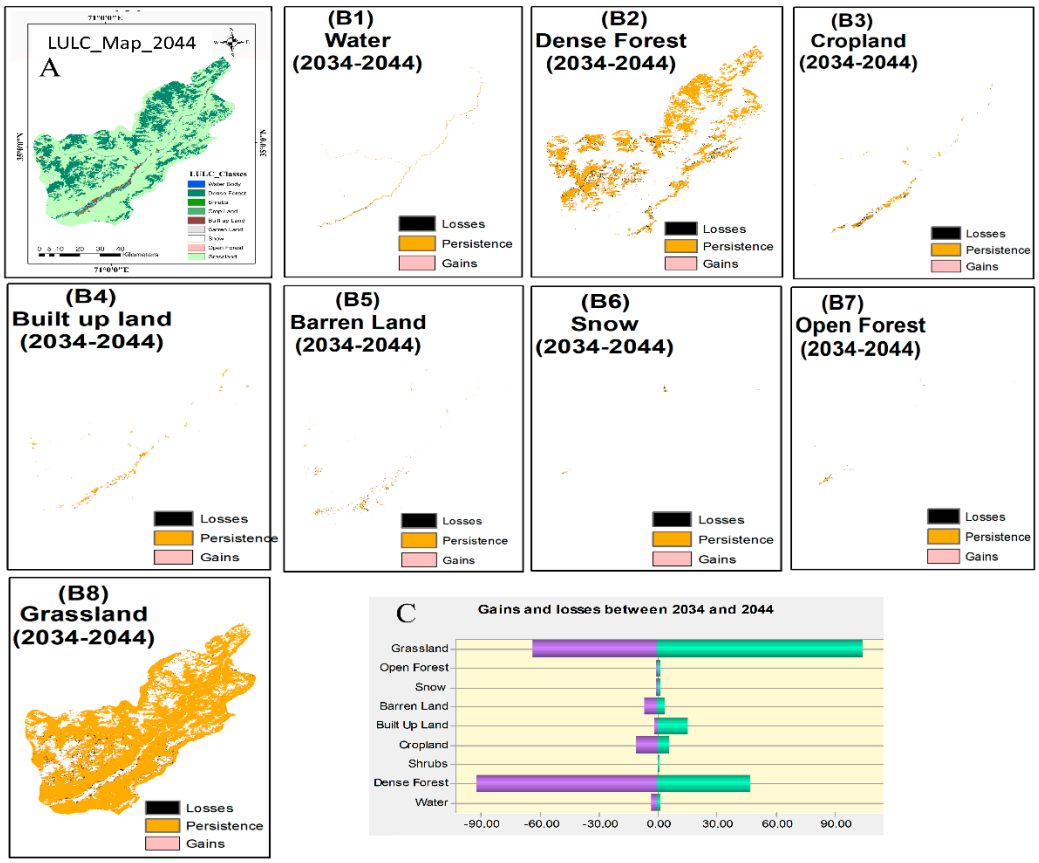

Figure 8. LULC dynamics and transition analysis in the study area from 2034 to 2044. (A) LULC classification map for the year 2044. (B1–B8) Spatial distribution of LULC transitions during the 2034–2044 period. (C) Gains and losses in area (km²) between 2034 and 2044.

3.9. Contributors to LULC Changes from 2024 to 2044

To analyze the transformations of various LULC types, the contributions of each class converted into other categories over the 20 years are expressed in km². Dense forests were the dominant driver of grassland expansion over the past two decades. Between 2024 and 2034, dense forest contributed approximately -11.53 km² to the increase in grassland (Table S6). From 2034 to 2044, dense forest contributed about -47.14 km². Other classes contributed 0-1 km². From 2024 to 2044, dense forests were the primary driver of grassland expansion in the study area (Figure S1).

3.10. LULC Dynamics Based on Transition Matrix Analysis (2024–2044)

The transition matrix analysis for 2024–2034 and 2034–2044 reveals considerable spatiotemporal shifts in LULC across the study region. A significant transformation is evident in forest and grassland classes, with dense forest areas progressively declining over time. Between 2024 and 2034, approximately 27 km² of dense forest transitioned into grassland, and this trend continued from 2034 to 2044, with an additional 46.64 km² being converted. These changes suggest increasing anthropogenic pressures on forested landscapes. From 2024 to 2034, cropland slightly decreased in area (~53.57 km²), suggesting that some cropland area was converted into built-up areas and grasslands. Similarly, built-up land expanded significantly, increasing from 52.16 km² in 2034 to 60.63 km² by 2044, with much of this growth sourced from former cropland and forest. Grassland demonstrated the largest areal extent among all LULC classes, maintaining dominance while gradually increasing coverage. For instance, grassland expanded by 3652.29 km² by 2034 and grew

 doi:10.20944/preprints202603.0530.v1

to 3690.25 km² by 2044. However, this increase often occurred at the cost of dense forests, open forests, and cropland, as indicated by conversion rates within the matrix (Table S7). The primary drivers behind these LULC dynamics appear to be illegal logging dense forests, notably the expansion of the timber industry. Urban growth, and a scarcity of employment opportunities have intensified socio-economic pressures on the landscape, especially close to the forest areas. Additionally, unsustainable practices such as local communities' use of firewood and charcoal for household energy, have exacerbated forest degradation [62]. Unregulated and informal settlements have also contributed to the degradation of forests [63]. Effective land-use planning and strict forest management policies are urgently needed to mitigate these adverse impacts. Restoration initiatives, including the government's current afforestation and reforestation programs, may help reverse some of the damage. If implemented systematically, these programs could restore previously deforested areas and balance future LULC changes. The transition matrices (Table S7) depict how the expansion of one land cover type often occurs at the expense of another, underlining the critical need for an integrated landscape management approach in future planning scenarios

3.11. Impact of LULC Changes on Forests

Many countries, including Afghanistan, are increasingly vulnerable to LULC changes, which have significant environmental and socio-economic implications [13]. These transformations exert increasing pressure on the environment, particularly in forests. Forest degradation can lead to the deterioration of critical landscape components, such as flora and fauna, resulting in desertification and negative consequences like biodiversity loss and health issues [64]. Deforestation, a significant LULC change, is a primary factor influencing hydrological processes, including surface runoff, evapotranspiration, groundwater, infiltration, lateral flow, and rainfall interception [65]. Human activity, particularly in Afghanistan's border areas, drives LULC changes that, in turn, affect the availability of forest resources and the health of the ecosystem [66]. Kunar province, a crucial area in Eastern Afghanistan, hosts one of the densest forest ecosystems in the region [28]. Land use and climate change are the primary factors influencing the forest ecosystems [67]. Future forest health is closely tied to effective land-use management and planning, particularly as population growth and grassland expansion place greater demands on the land. These factors contribute to reduced forest cover and biodiversity, weakening the ecosystem's resilience. Forest loss exacerbates evapotranspiration, reduces baseflow, and diminishes groundwater, thereby affecting forest regeneration and water retention capacity [68]. Consequently, ongoing forest degradation heightens concern about forest health and ecosystem sustainability. Land use changes, such as fragmentation and degradation, negatively impact forest ecosystems, reducing their capacity to absorb carbon and produce oxygen [69]. These changes also contribute to the displacement of sediment and chemicals, polluting the surrounding environment. Forest degradation in the study area is linked to the release of greenhouse gases such as methane and CO_2, further harming the atmosphere [22]. This study highlights a direct relationship between LULC changes and forest health, with deforestation being a key contributor to the adverse effects on forest biodiversity. To safeguard the future health of forest ecosystems in the study area, it is crucial to implement strategic land-use management practices and mitigate the impacts of ongoing land-use changes.

4. Conclusions

To effectively shape future policies and strategies for land management and conservation, it is crucial to understand the dynamics of natural resource changes and project future scenarios. In this study, the CA-Markov model was employed to simulate future land use patterns for 2034 and 2044 in the study area. These predictions were based on historical land-use maps from 2004, 2014, and 2024, and the model's validity was confirmed by comparing the simulated 2024 LULC map with the current 2024 map. Following successful validation, projections for 2034 and 2044 were also made. The results from model validation demonstrated that the LCM effectively predicts future LULC states with an accuracy exceeding 80%, the minimum acceptable threshold. The analysis of land use

 doi:10.20944/preprints202603.0530.v1

changes between 2004 and 2024 revealed significant increases in grassland and notable losses in dense forest and cropland areas. By 2044, grassland is expected to expand by 0.7%, while dense forest is expected to decline by -1.15%. The observed loss in dense forest is primarily attributed to grassland expansion. Future projections show a continued rise in grassland and built-up areas, encroaching further on dense forest and cropland regions. This trend is primarily influenced by population growth and the rising demand for livelihood sources, which has led to the gradual clearing of forested areas and their subsequent conversion into grassland. The conversion of dense forests into grassland across the area poses a critical concern for forest sustainability. This transition is expected to increase soil erosion, reduce biodiversity, and affect ecosystem functions, such as carbon sequestration and soil stability. The study underscores the link between land use changes and the overall health of forest ecosystems, with significant implications for biodiversity conservation and ecosystem services. In areas such as eastern Afghanistan, understanding historical and projected land-use patterns is essential for managing forest resources and ensuring long-term sustainability. Policymakers must implement timely and effective forest management practices to mitigate these changes and promote sustainable growth. These findings offer valuable insights into the long-term management of forest ecosystems in the study area and provide a solid foundation for addressing future challenges in forest conservation and land-use planning.

Supplementary Materials: The following supporting information can be downloaded at the website of this paper posted on Preprints.org.

Author Contributions: Conceptualization, B.J.H.M; methodology, B.J.H.M. and M.J.M; formal analysis, B.J.H.M; Writing-Original draft preparation, L.D. and A.C.T; writing reviewing, A.C.T; Data Interpretation and editing, L.D and A.C.T.

Funding: This study did not receive any specific funding.

Data Availability Statement: All Landsat imagery was obtained from the USGS website (https://earthexplorer.usgs.gov) as well as Google Earth Engine (https://earthengine.google.com).

Acknowledgments: The authors acknowledge financial support for the Institute of Earth Sciences (ICT) from the Foundation for Science and Technology (FCT) through the funding contract, under project UID/04683 (DOI: 10.54499/UID/PRR/04683/2025).

Conflicts of Interest: The authors declare no conflict of interest.

References

1. Heal, K., *Watershed management in action: lessons learned from FAO field projects.* Mountain Research and Development, 2019. **39**(1): p. M5-M6.
2. Mmbaga, N.E., L.K. Munishi, and A.C. Treydte, *How dynamics and drivers of land use/land cover change impact elephant conservation and agricultural livelihood development in Rombo, Tanzania.* Journal of Land Use Science, 2017. **12**(2-3): p. 168-181.
3. Ren, Y., et al., *Spatially explicit simulation of land use/land cover changes: Current coverage and future prospects.* Earth-Science Reviews, 2019. **190**: p. 398-415.
4. Yesuph, A.Y. and A.B. Dagnew, *Land use/cover spatiotemporal dynamics, driving forces and implications at the Beshillo catchment of the Blue Nile Basin, North Eastern Highlands of Ethiopia.* Environmental Systems Research, 2019. **8**(1): p. 1-30.
5. De La Fuente, B., et al., *Built-up areas within and around protected areas: Global patterns and 40-year trends.* Global ecology and conservation, 2020. **24**: p. e01291.
6. Phommavong, K., J. Yan, and S.A. Shah, *Assessment of urban growth patterns on forest and water resources changes using remote sensing and machine learning techniques.* Journal of Water and Climate Change, 2025. **16**(11): p. 3308-3328.
7. Sarfo, I., et al., *CAUSAL EFFECTS AND PREDICTION OF LAND USE SYSTEMS IN RURAL LANDSCAPES: EVIDENCE FROM HENAN PROVINCE.* Acta Scientiarum Polonorum. Formatio Circumiectus, 2024. **23**(3).

 doi:10.20944/preprints202603.0530.v1

8. Gitz, V., et al., *Climate change and food security: risks and responses.* Food and Agriculture Organization of the United Nations (FAO) Report, 2016. **110**(2): p. 3-36.
9. Zhang, C. and X. Li, *Land use and land cover mapping in the era of big data.* Land, 2022. **11**(10): p. 1692.
10. Tavares, P.A., et al., *Integration of sentinel-1 and sentinel-2 for classification and LULC mapping in the urban area of Belém, eastern Brazilian Amazon.* Sensors, 2019. **19**(5): p. 1140.
11. Mohajane, M., et al., *Land use/land cover (LULC) using landsat data series (MSS, TM, ETM+ and OLI) in Azrou Forest, in the Central Middle Atlas of Morocco.* Environments, 2018. **5**(12): p. 131.
12. Gibbs, H.K., et al., *Tropical forests were the primary sources of new agricultural land in the 1980s and 1990s.* Proceedings of the National Academy of Sciences, 2010. **107**(38): p. 16732-16737.
13. Najmuddin, O., et al., *Valuation of land-use/land-cover-based ecosystem Services in Afghanistan—An Assessment of the past and future.* Land, 2022. **11**(11): p. 1906.
14. Hekmat, H., et al., *Land use and land cover changes in Kabul, Afghanistan focusing on the drivers impacting urban dynamics during five decades 1973–2020.* Geomatics, 2023. **3**(3): p. 447-464.
15. Riad, P., et al., *Landscape transformation processes in two large and two small cities in Egypt and Jordan over the last five decades using remote sensing data.* Landscape and Urban Planning, 2020. **197**: p. 103766.
16. Tarasovičová, Z., et al., *Changes in agricultural land use in the context of ongoing transformational processes in Slovakia.* Agriculture (Pol'nohospodárstvo), 2013. **59**(2): p. 49-64.
17. Sharma, A.K., et al., *Assessment of land use change and climate change impact on biodiversity and environment*, in *Environmental pollution and natural resource management*. 2022, Springer. p. 73-89.
18. Wang, J., et al., *Machine learning in modelling land-use and land cover-change (LULCC): Current status, challenges and prospects.* Science of the Total Environment, 2022. **822**: p. 153559.
19. Ahmad, M.N., Z. Shao, and A. Javed, *Modelling land use/land cover (LULC) change dynamics, future prospects, and its environmental impacts based on geospatial data models and remote sensing data.* Environmental Science and Pollution Research, 2023. **30**(12): p. 32985-33001.
20. Gaur, S. and R. Singh, *A comprehensive review on land use/land cover (LULC) change modeling for urban development: current status and future prospects.* Sustainability, 2023. **15**(2): p. 903.
21. Noszczyk, T., *A review of approaches to land use changes modeling.* Human and Ecological Risk Assessment: An International Journal, 2018.
22. Arfasa, G.F., E. Owusu-Sekyere, and D.A. Doke, *Predictions of land use/land cover change, drivers, and their implications on water availability for irrigation in the Vea catchment, Ghana.* Geocarto International, 2023. **38**(1): p. 2243093.
23. Mishra, V.N. and P.K. Rai, *A remote sensing aided multi-layer perceptron-Markov chain analysis for land use and land cover change prediction in Patna district (Bihar), India.* Arabian Journal of Geosciences, 2016. **9**: p. 1-18.
24. Zadbagher, E., K. Becek, and S. Berberoglu, *Modeling land use/land cover change using remote sensing and geographic information systems: case study of the Seyhan Basin, Turkey.* Environmental monitoring and assessment, 2018. **190**: p. 1-15.
25. Girma, R., C. Fürst, and A. Moges, *Land use land cover change modeling by integrating artificial neural network with cellular Automata-Markov chain model in Gidabo river basin, main Ethiopian rift.* Environmental Challenges, 2022. **6**: p. 100419.
26. Eastman, J.R., *Idrisi selva tutorial.* Idrisi Production, Clark Labs-Clark University, 2012. **45**(January): p. 51-63.
27. Leta, M.K., T.A. Demissie, and J. Tränckner, *Modeling and prediction of land use land cover change dynamics based on land change modeler (Lcm) in nashe watershed, upper blue nile basin, Ethiopia.* Sustainability, 2021. **13**(7): p. 3740.
28. Bader, H.R., et al., *Illegal timber exploitation and counterinsurgency operations in Kunar Province of Afghanistan: A case study describing the nexus among insurgents, criminal cartels, and communities within the forest sector.* Journal of sustainable forestry, 2013. **32**(4): p. 329-353.
29. Hosseini, F.S., et al., *Spatial prediction of physical and chemical properties of soil using optical satellite imagery: a state-of-the-art hybridization of deep learning algorithm.* Frontiers in Environmental Science, 2023. **11**: p. 1279712.

 doi:10.20944/preprints202603.0530.v1

30. Mashkoor, R., et al., *Detecting Li-bearing pegmatites using geospatial technology: the case of SW Konar Province, Eastern Afghanistan.* Geocarto International, 2022. **37**(26): p. 14105-14126.
31. Abdullah, S., V. Chmyriov, and V. Dronov, *Geology and mineral resources of Afghanistan.* 2008.
32. Nagra, G.M., et al., *People, Politics, and Society: A Historical Analysis of Afghanistan.* Remittances Review, 2024. **9**(2): p. 539-556.
33. Sen, P.C., M. Hajra, and M. Ghosh, *Supervised classification algorithms in machine learning: A survey and review*, in *Emerging technology in modelling and graphics: Proceedings of IEM graph 2018*. 2019, Springer. p. 99-111.
34. Amaechi, C., O. Ogbemudia, and A. Okoduwa, *LAND USE/LAND COVER CHANGE PROJECTION FOR THE YEAR 2050: AN ASSESSMENT OF LAGOS STATE, NIGERIA.* Ethiopian Journal of Environmental Studies & Management, 2024. **17**(2).
35. Jenness, J. and J.J. Wynne, *Cohen's Kappa and classification table metrics 2.0: an ArcView 3x extension for accuracy assessment of spatially explicit models*. 2005.
36. Hussain, K., et al., *Analysing LULC transformations using remote sensing data: insights from a multilayer perceptron neural network approach.* Annals of GIS, 2024: p. 1-28.
37. Hansen, R.E., *Change detection on shipwrecks using synthetic aperture sonar–North Sea Wrecks Task 3.5 Deep Water Case Study*. 2022.
38. Islam, K., M.F. Rahman, and M. Jashimuddin, *Modeling land use change using cellular automata and artificial neural network: The case of Chunati Wildlife Sanctuary, Bangladesh.* Ecological indicators, 2018. **88**: p. 439-453.
39. Hitouri, S., et al., *Hybrid machine learning approach for gully erosion mapping susceptibility at a watershed scale.* ISPRS International Journal of Geo-Information, 2022. **11**(7): p. 401.
40. Kelley, K., *The average rate of change for continuous time models.* Behavior Research Methods, 2009. **41**(2): p. 268-278.
41. Xing, H., Y. Meng, and Y. Shi, *A dynamic human activity-driven model for mixed land use evaluation using social media data.* Transactions in GIS, 2018. **22**(5): p. 1130-1151.
42. Hamad, R., H. Balzter, and K. Kolo, *Predicting land use/land cover changes using a CA-Markov model under two different scenarios.* Sustainability, 2018. **10**(10): p. 3421.
43. Roy, D.P., et al., *Landsat-8: Science and product vision for terrestrial global change research.* Remote sensing of Environment, 2014. **145**: p. 154-172.
44. Pérez-Vega, A., J.-F. Mas, and A. Ligmann-Zielinska, *Comparing two approaches to land use/cover change modeling and their implications for the assessment of biodiversity loss in a deciduous tropical forest.* Environmental Modelling & Software, 2012. **29**(1): p. 11-23.
45. Megahed, Y., et al., *Land cover mapping analysis and urban growth modelling using remote sensing techniques in Greater Cairo Region—Egypt.* ISPRS International Journal of Geo-Information, 2015. **4**(3): p. 1750-1769.
46. Mahmoud, S.H. and A. Alazba, *Land cover change dynamics mapping and predictions using EO data and a GIS-cellular automata model: the case of Al-Baha region, Kingdom of Saudi Arabia.* Arabian journal of geosciences, 2016. **9**: p. 1-20.
47. Larbi, I., et al., *Predictive land use change under business-as-usual and afforestation scenarios in the vea catchment, West Africa*. 2019.
48. Eastman, J.R. and J. Toledano, *A short presentation of the Land Change Modeler (LCM).* Geomatic approaches for modeling land change scenarios, 2018: p. 499-505.
49. Beroho, M., et al., *Future scenarios of land use/land cover (LULC) based on a CA-markov simulation model: case of a mediterranean watershed in Morocco.* Remote Sensing, 2023. **15**(4): p. 1162.
50. Fathizad, H., N. Rostami, and M. Faramarzi, *Detection and prediction of land cover changes using Markov chain model in semi-arid rangeland in western Iran.* Environmental monitoring and assessment, 2015. **187**: p. 1-12.
51. Singh, S.K., et al., *Predicting spatial and decadal LULC changes through cellular automata Markov chain models using earth observation datasets and geo-information.* Environmental Processes, 2015. **2**: p. 61-78.
52. Zhang, C.-L., et al., *Effect of neurolytic celiac plexus block guided by computerized tomography on pancreatic cancer pain.* Digestive diseases and sciences, 2008. **53**: p. 856-860.
53. Zhou, X. and H. Chen, *Impact of urbanization-related land use land cover changes and urban morphology changes on the urban heat island phenomenon.* Science of the Total Environment, 2018. **635**: p. 1467-1476.

 doi:10.20944/preprints202603.0530.v1

54. Vázquez-Quintero, G., et al., *Detection and projection of forest changes by using the Markov Chain Model and cellular automata.* Sustainability, 2016. **8**(3): p. 236.
55. Gharaibeh, A., et al., *Improving land-use change modeling by integrating ANN with Cellular Automata-Markov Chain model.* Heliyon, 2020. **6**(9).
56. Qasim, M., et al., *Modelling land use change across elevation gradients in district Swat, Pakistan.* Regional environmental change, 2013. **13**: p. 567-581.
57. Mahamud, M., et al., *Prediction of future land use land cover changes of Kelantan, Malaysia.* The International Archives of the Photogrammetry, Remote Sensing and Spatial Information Sciences, 2019. **42**: p. 379-384.
58. Muhammad, R., et al., *Spatiotemporal change analysis and prediction of future land use and land cover changes using QGIS MOLUSCE plugin and remote sensing big data: a case study of Linyi, China.* Land, 2022. **11**(3): p. 419.
59. Wu, K.-y. and H. Zhang, *Land use dynamics, built-up land expansion patterns, and driving forces analysis of the fast-growing Hangzhou metropolitan area, eastern China (1978–2008).* Applied geography, 2012. **34**: p. 137-145.
60. Kafy, A.-A., et al., *Geospatial approach for developing an integrated water resource management plan in Rajshahi, Bangladesh.* Environmental Challenges, 2021. **4**: p. 100139.
61. Mishra, K., L. Boynton, and A. Mishra, *Driving employee engagement: The expanded role of internal communications.* International Journal of Business Communication, 2014. **51**(2): p. 183-202.
62. Ullah, A., *Community and Institutional Drivers of Deforestation, Environmental Impacts, and Extension Interventions for Forest Management in the Hindu Kush Himalaya.* Land Degradation & Development, 2025.
63. Roberts, R.E. and O. Okanya, *Measuring the socio–economic impact of forced evictions and illegal demolition; A comparative study between displaced and existing informal settlements.* The Social Science Journal, 2022. **59**(1): p. 119-138.
64. Ekka, P., et al., *Land Degradation and its impacts on Biodiversity and Ecosystem services.* Land and Environmental Management through Forestry, 2023: p. 77-101.
65. Panda, S., et al., *Geospatial technology applications in forest hydrology*, in *Forest hydrology: processes, management and assessment*. 2016, CABI Wallingford UK. p. 162-179.
66. Hussain, K., et al., *Animals Feed in Transition: Intricate Interplay of Land Use Land Cover Change and Fodder Sources in Kurram Valley, Pakistan.* Resources (2079-9276), 2024. **13**(2).
67. Tian, L., et al., *Dynamic simulation of land use/cover change and assessment of forest ecosystem carbon storage under climate change scenarios in Guangdong Province, China.* Remote Sensing, 2022. **14**(10): p. 2330.
68. Krishnaswamy, J., et al., *The groundwater recharge response and hydrologic services of tropical humid forest ecosystems to use and reforestation: Support for the "infiltration-evapotranspiration trade-off hypothesis".* Journal of Hydrology, 2013. **498**: p. 191-209.
69. Sonwa, D.J., et al., *Vulnerability, forest-related sectors and climate change adaptation: The case of Cameroon.* Forest Policy and Economics, 2012. **23**: p. 1-9.